AD

Reports Control Symbol
OSD-1366

RESEARCH AND DEVELOPMENT TECHNICAL REPORT
ECOM-5531

ATMOSPHERIC EFFECTS FOR GROUND TARGET SIGNATURE MODELING

II. Discussion and Application of a Generalized Molecular Absorption Model

By

James B. Gillespie

Carmine Petracca

Atmospheric Sciences Laboratory
US Army Electronics Command
White Sands Missile Range, New Mexico 88002

January 1974

Approved for public release; distribution unlimited.

ECOM

UNITED STATES ARMY ELECTRONICS COMMAND - FORT MONMOUTH, NEW JERSEY 07703

NOTICES

Disclaimers

The findings in this report are not to be construed as an official Department of the Army position, unless so designated by other authorized documents.

The citation of trade names and names of manufacturers in this report is not to be construed as official Government indorsement or approval of commercial products or services referenced herein.

Disposition

Destroy this report when it is no longer needed. Do not return it to the originator.

UNCLASSIFIED

SECURITY CLASSIFICATION OF THIS PAGE (When Data Entered)

REPORT DOCUMENTATION PAGE

READ INSTRUCTIONS BEFORE COMPLETING FORM

1. REPORT NUMBER: ECOM-5531
2. GOVT ACCESSION NO.
3. RECIPIENT'S CATALOG NUMBER
4. TITLE (and Subtitle): ATMOSPHERIC EFFECTS FOR GROUND TARGET SIGNATURE MODELING. II. DISCUSSION AND APPLICATION OF A GENERALIZED MOLECULAR ABSORPTION MODEL
5. TYPE OF REPORT & PERIOD COVERED
6. PERFORMING ORG. REPORT NUMBER
7. AUTHOR(s): James B. Gillespie and Carmine Petracca
8. CONTRACT OR GRANT NUMBER(s)
9. PERFORMING ORGANIZATION NAME AND ADDRESS: Atmospheric Sciences Laboratory, White Sands Missile Range, New Mexico 88002
10. PROGRAM ELEMENT, PROJECT, TASK AREA & WORK UNIT NUMBERS: DA Task No. 1T061102B53A-19
11. CONTROLLING OFFICE NAME AND ADDRESS: US Army Electronics Command, Fort Monmouth, New Jersey 07703
12. REPORT DATE: January 1974
13. NUMBER OF PAGES: 33
14. MONITORING AGENCY NAME & ADDRESS (if different from Controlling Office)
15. SECURITY CLASS. (of this report): Unclassified
15a. DECLASSIFICATION/DOWNGRADING SCHEDULE
16. DISTRIBUTION STATEMENT (of this Report): Approved for public release; distribution unlimited.
17. DISTRIBUTION STATEMENT (of the abstract entered in Block 20, if different from Report)
18. SUPPLEMENTARY NOTES
19. KEY WORDS (Continue on reverse side if necessary and identify by block number)

1. Band Models
2. Molecular Absorption
3. Transmission
4. Attenuation

20. ABSTRACT (Continue on reverse side if necessary and identify by block number)

This report is a detailed discussion of the five-parameter generalization of the Zachor molecular absorption model proposed by Gibson and Pierluissi, and applies that model to a horizontal path of water vapor data. This application covers the spectral intervals of 1200 to 2200 cm^{-1} and 4900 to 5800 cm^{-1} with a resolution of 50 cm^{-1}. The five parameters of the model are determined for each frequency, and the transmission is calculated and plotted. The results of this application are then qualitatively compared to results obtained from the modified

DD FORM 1 JAN 73 1473 EDITION OF 1 NOV 65 IS OBSOLETE

UNCLASSIFIED

SECURITY CLASSIFICATION OF THIS PAGE (When Data Entered)

20.

King's function which is utilized in the Air Force Cambridge Research Laboratory (AFCRL) transmittance model.

In the 1200-1850 cm^{-1} and the 5100-5800 cm^{-1} intervals, the two models predict generally similar though not identical results; they predict markedly different results in the 1850-2200 cm^{-1} and 4900-5100 cm^{-1} intervals.

The transmittance values calculated with the use of these models are compared to the original data which were used in the development of the models. The five-parameter model reproduces the data of Wyatt et al. to within 0.5%, while the modified King's function model reproduces the published data of Burch et al. to within 10%.

AD-774254

PREFACE

The objective of the Atmospheric Sciences Laboratory (ASL) effort within the Ground Target Signature (GTS) program is to develop a total atmospheric transmission model that takes into account molecular and aerosol scattering and absorption. The five-parameter generalization of the Zachor molecular absorption model originally proposed by Gibson and Pierluissi in 1971 is in the process of being integrated into a comprehensive ASL transmittance model. This absorption model is reviewed and compared with the modified King's function model used in the Air Force Cambridge Research Laboratory (AFCRL) model presently being used for GTS purposes. Since further improvements need to be made to develop the five-parameter model for general use, additional work to improve the model and refine the computer techniques involved is being done under contract number DDAD07-73-C-0127 at the University of Texas at El Paso by Joseph Pierluissi, Leland Blank, and Jerry Collins. This work includes applying the model to high resolution data, extending the use of the model to real atmospheric conditions, applying inhomogeneous path techniques, and improving the computer program efficiency.

The authors gratefully acknowledge the cooperation and assistance of Glenn A. Gibson and Joseph H. Pierluissi of the University of Texas at El Paso. We also wish to acknowledge the relevant discussions with John E. Selby of AFCRL concerning the application of the modified King's function model. We especially wish to acknowledge Richard B. Gomez for his critical review and his many helpful suggestions.

CONTENTS

INTRODUCTION

This is the second in a series of reports to determine a total atmospheric transmittance model for the Ground Target Signatures (GTS) program. Gomez and Pierluissi [1] reviewed the state-of-the-art of calculating atmospheric transmission, and recommended that a generalized molecular absorption model be considered as potentially the best model available for treating broad band atmospheric absorption.

This report discusses and applies the five-parameter generalization of Zachor's model [2], henceforth referred to as the FP(five-parameter) model. This application is to a 1-km horizontal path of water vapor data calculated by Wyatt, Stull, and Plass [3] over spectral intervals of 1200 to 2200 cm^{-1} and 4900 to 5800 cm^{-1} with a resolution of 50 cm^{-1}. To provide a basis of comparison, a modified King's function (MKF) absorption model, used by Air Force Cambridge Research Laboratories (AFCRL) in their total atmospheric transmission model [4], is applied to the same path and spectral intervals using the water vapor data of Burch, Singleton, France, and Williams [5] degraded to a resolution of 50 cm^{-1}.

The AFCRL model was chosen as a basis of comparison because it is used in GTS applications.

DISCUSSION OF THE FIVE-PARAMETER MODEL

Development of the Five-Parameter Model

The FP band model discussed in this paper is a quadratic generalization of the four-parameter absorption model developed by Zachor [2, 6]. As originally proposed by Gibson and Pierluissi [7], it was developed by considering the Zachor model as the equation of an elliptic cone and writing that expression as a more general three-term polynomial equation. The Zachor model is a modification of the Mayer-Goody statistical band model for gaseous transmittance. The Mayer-Goody model is [8, 9]:

$$\tau = \exp\left[\frac{-q}{\left(1 + \frac{2q}{\beta}\right)}\right]^{\frac{1}{2}} \qquad (1)$$

where

τ = transmission

q = $SU/d = kU$

U = optical path length

k = absorption coefficient

S = spectral line intensity

d = mean spacing between spectral lines

β = $2\pi\gamma/d = \beta_o P$

β_o = β calculated at standard temperature and pressure

γ = spectral line half-width

P = gaseous broadening pressure

Eq. (1) may be rewritten as

$$\tau = \exp\left[-\left(\frac{1}{q^2} + \frac{2}{q\beta}\right)^{-\frac{1}{2}}\right] \tag{2}$$

or

$$\tau = \exp\left[-\left(\frac{1}{(kU)^2} + \frac{2}{CUP}\right)^{-\frac{1}{2}}\right] \tag{3}$$

where $C = \beta_o k$ is the proportionality factor between UP and $q\beta$ and is frequency-dependent. The product CUP is used instead of $q\beta$ because q and β cannot be directly measured.

For $U/P \ll 1$, the weak-line approximation, Eq. (3) reduces to

$$\tau_w = \exp(-kU) \tag{4}$$

and for $U/P \gg 1$, the strong-line approximation, Eq. (3) reduces to

$$\tau_s = \exp\left[-\left(\frac{CUP}{2}\right)^{\frac{1}{2}}\right] \tag{5}$$

Combining Eqs. (3), (4), and (5), the Mayer-Goody model may be rewritten as

$$(\ln\tau)^{-2} = (\ln\tau_w)^{-2} + (\ln\tau_s)^{-2} \tag{6}$$

Zachor [2] noted that this equation may be regarded geometrically as the resultant magnitude of two perpendicular vectors of lengths $(\ln \tau_w)^{-1}$ and $(\ln \tau_s)^{-1}$, as shown in Figure 1(a). Extending this geometric interpretation and applying the cosine law, he proposed a more general model which may be expressed as

$$Z^2 = \left(\frac{1}{k^2}\right) x^2 + y^2 - \left(\frac{M}{k}\right) xy \tag{7}$$

where

$Z = 1/\ln \tau$

$x = 1/U$

$y = 1/\ln \tau_s$

$M = 2 \cos \theta$

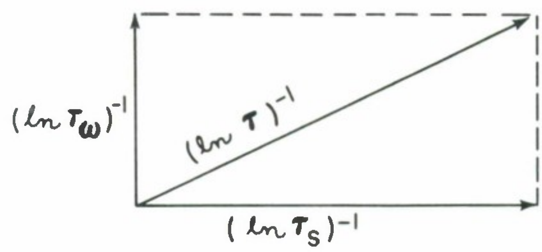

Figure 1a. The vector representation of the Mayer-Goody model.

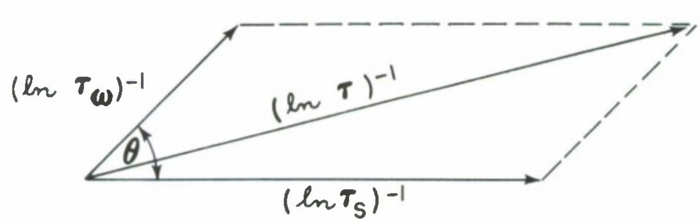

Figure 1b. The vector representation of the Zachor model.

$(\ln \tau)^{-1}$ is now the sum of two vectors, $(\ln \tau_W)^{-1}$ and $(\ln \tau_S)^{-1}$, whose directions differ by a fixed angle θ, as shown in Figure 1(b). The value θ has no effect on the value of τ; however, it does control the rate of transition between τ_W and τ_S. The cross term can thus be interpreted as representing the region of intermediate absorption.

The Zachor formula, when written in the form of Eq. (7), is the equation of an elliptic cone. The ellipse is in the xy-plane, and the xy term corresponds to a rotation of the ellipse about the z-axis. Since $M = 2 \cos \theta$, M will be less than or equal to 2. This restriction guarantees that the cone will be elliptic (or parabolic for $|M| = 2$). This comes from the restriction in analytic geometry that $A_3^2 < 4A_1A_2$, where A_1 is the coefficient of x^2, A_2 is the coefficient of y^2, and A_3 is the coefficient of xy.

To use the analytical models described above, one essentially determines an elliptic cone that best fits the data points (x_i, y_i, z_i). This may be done by using minimization techniques to weight the terms of the equation of the ellipse. The coefficients are determined from the resulting best fit. This procedure must then be repeated for each frequency, since the parameters are frequency-dependent.

Using the observations presented above, Gibson and Pierluissi [7] proposed a generalized polynomial model which would allow for complete flexibility in weighting the terms of the equation. The proposed model is

$$Z^2 = B_W X^2 + B_S Y^2 + B_{WS} XY \tag{8}$$

where B_W is the frequency-dependent parameter which weights the weak-line transmission with respect to the other two terms. It is not necessarily $(1/K^2)$, as in the Zachor model. B_S is the frequency-dependent parameter which weights the strong-line transmission terms. B_{WS} is the frequency-dependent parameter which weights the transition between x and y. These coefficients satisfy the condition $B_{WS}^2 < 4B_W B_S$.

In a later paper Pierluissi [10] further generalizes the model and describes the general polynomial transmission model as

$$Z^2 = B_w X^2 + B_s Y^2 + B_{ws} XY + B_{3ws} X^2 Y + B_{2ws} XY^2 + \ldots \tag{9}$$

in which the right side of the equation is simply an n-order polynomial given by the expression

$$F(x, y) = \sum_{n}^{\infty} \sum_{i}^{\infty} B_{n_i} X^n Y^i \tag{10}$$

The first order terms of Eq. (10) correspond to a translation of the x- and y-axes and may be removed by algebraic methods. The accuracy produced by the third order and higher terms is not needed for general atmospheric transmittance modeling, and the inclusion of these terms results in greater complexity of the model and more computational effort. Eq. (9) is therefore truncated after the first three terms, yielding Eq. (8). As more terms are used, the coefficients lose their physical meaning.

As written, the Zachor model, Eq. (7), and the FP model, Eq. (8), have only two and three explicit parameters, respectively. However, both models use the two-parameter strong-line transmission function proposed by King [11] for their representations of τ_s. King's formula is

$$\tau_s = 1 - P\{n, [n\Gamma(n) (\frac{2CUP}{\pi})^{\frac{1}{2}}]^{1/n}\} \tag{11}$$

where P(a, x) is the incomplete gamma function

$$P(a, x) = [\Gamma(a)]^{-1} \int_0^x t^{a-1} e^{-t} dt \qquad (12)$$

King developed his strong-line transmission model based on the fact that the character of the line spacing is the most important factor in the transmittance of overlapping spectral lines. He compared the transmittance of the Elsasser model to the transmittance of the Mayer-Goody model and found no relationship between the two; however, in taking the derivatives of the absorptances of the models with respect to the absorber quantity, he discovered a relationship which led him to formulate two important assumptions: (1) The absorption derivative of widely spaced overlapping Lorentz lines can be expressed as the product of the absorption derivative of the lines considered as non-interacting absorbers and an overlap factor which involves the interaction of the neighboring lines. (2) For widely spaced Lorentz absorption lines, the overlap factor can be expressed as an exponential function in which the power of the argument is related to the variance of the line spacing. The assumptions form the basis for the derivation of King's formula.

Eq. (11) has two frequency-dependent parameters, n and C. The parameter n is an adjustable strong-line parameter which controls the ratio of the variance, σ^2, and the squared mean of the line spacing, d^2, for widely spaced, equally intense strong lines, as in the probability density function [6]:

$$\frac{\sigma^2}{d^2} = \{2n\Gamma(2n)/[n\Gamma(n)]^2\}-1 \qquad (13)$$

The Mayer-Goody model (Poisson-distributed lines) is characterized by unit variance, while the Elsasser model (regularly spaced lines) is characterized by zero variance. For Poisson-distributed lines (n = 1), Eq. (13) gives the correct result; however, for regularly spaced lines

($n = \frac{1}{2}$), it gives $\sigma^2/d^2 = (4/\pi - 1)$ instead of zero. Nevertheless, King's formula, Eq. (11), is very useful because it provides a continuous set of trial functions for fitting strong-line data, and it reduces to the Elsasser strong-line approximation for $n = \frac{1}{2}$ and to the Mayer-Goody strong line approximation for $n = 1$. For $n > 1$, the expression represents clustering of spectral lines. Eq. (11) is thus a generalized strong-line absorption model whose line spacing goes from complete regularity to complete randomness and to the limit of clustering in which the spectral lines are superimposed upon one another.

The parameter C is a strong-line parameter related to the line spacing, d, the line strength, S, and the half-width, γ_o, of the spectral lines by

$$C = \frac{2\pi\gamma_o S}{d^2} \tag{14}$$

With King's strong-line transmission function (Eq. (11)) incorporated into Eq. (8), the proposed model becomes a five-parameter model (n, C, B_w, B_s, B_{ws}). All five parameters must be calculated for each frequency. The techniques used to determine these parameters will be discussed in the next section.

That the FP model is indeed a very general and very useful analytical model can be shown in that at least nine other models can be derived from it by forcing the parameter to certain values [12].

The models that can be obtained are:

1. Beer's Law. By setting $B_s = B_{ws} = 0$ and $B_w = 1/k^2$, we obtain $\tau = e^{-kU}$.

2. King's Strong-line Model. By setting $B_w = B_{ws} = 0$ and $B_s = 1$, we obtain Eq. (11), repeated here for convenience.

$$\tau_s = 1 - P\{n, \Gamma[n\tau(n)\ (\frac{2CUP}{\pi})^{\frac{1}{2}}]^{1/n}\}$$

3. Elsasser's Strong-line Approximation. By setting $B_w = B_{ws} = 0$, $B_s = 1$, and $n = 0.5$, we obtain

$$\tau = 1 - \frac{1}{\sqrt{\pi}} \Gamma[\tfrac{1}{2}, (\frac{CUP}{2})^{\frac{1}{2}}] \tag{15}$$

$$= 1 - \mathrm{erf}\,(\frac{CUP}{2})^{\frac{1}{2}}$$

4. The Mayer-Goody Strong-line Approximation. By setting $B_w = B_{ws} = 0$, $B_s = 1$, and $n = 1$, we obtain

$$\tau = 1 - P\,\{1, (\frac{2CUP}{\pi})^{\frac{1}{2}}\}$$

$$= \exp\,[-(\frac{2CUP}{\pi})^{\frac{1}{2}}] \tag{16}$$

5. The Mayer-Goody Model. By setting $B_{ws} = 0$, $B_s = 1$, $B_w = 1/k^2$, and $n = 1$, we obtain Eq. (3), repeated here.

$$\tau = \exp\,[-(\frac{1}{(kU)^2} + \frac{2}{CUP})^{\frac{1}{2}}]$$

6. The Generalized Mayer-Goody. By setting $B_{ws} = 0$ and using King's expression for τ_s with n variable, we obtain

$$(\ln\tau)^{-2} = \frac{1}{(kU)^2} + (\ln\tau_s)^{-2} \tag{17}$$

7. The Modified Elsasser. Setting $B_{ws} = 0$ and $n = \frac{1}{2}$, we obtain

$$(\ln\tau)^{-2} = \frac{1}{(kU)^2} + [1-\mathrm{erf}(\frac{CUP}{2})^{\frac{1}{2}}]^{-2} \quad (18)$$

8. Zachor's Model. By setting $B_s = 1$, $B_{ws} = M/k$, and $B_w = 1/k^2$, we obtain

$$(\ln\tau)^{-2} = \frac{1}{(kU)^2} + (\ln\tau_s)^{-2} - \frac{M}{kU}(\ln\tau_s)^{-1} \quad (19)$$

9. Intermediate Absorption (any model). Setting $B_w = B_s = 0$, we obtain

$$\tau_I = B_{ws} \ln\tau_w \ln\tau_s \quad (20)$$

Since these other models can be derived from the FP model, once the FP model is computerized, one can, with appropriate fixing of parameters, obtain any of the above models for use in the calculation of gaseous transmittance. A reduction in the number of parameters will result in a decrease of computer time and of required computer storage; however, it will also result in a decrease in the accuracy of the model.

Mathematical Techniques Used to Determine the Five Parameters

The mathematical algorithms used by Gibson and Pierluissi to determine the five parameters will be discussed in this section. As mentioned in the previous section, the parameters are frequency-dependent and must be calculated for each frequency. Ideally, Eq. (8) should be minimized, solving for all five parameters simultaneously by using all the absorption data; however, such a technique has not been perfected.

A procedure similar to that used by Zachor [2] was used to determine the parameters. First the strong-line parameters, n and C, were determined. Then these values were used in calculating the quadratic parameters: B_w, B_s, and B_{ws}. A simplified flowchart illustrating the computer procedures described in this section is shown in Figure 2.

The procedure for determining n and C is based on the fact that for a fixed UP product, such as U/P>>1 (the strong-line approximation), the absorptance must approach an upper limit of $1-\tau_s$, where τ_s is the strong-line transmittance. The strong-line parameters can thus be determined from the experimental data by plotting log $(1-\tau_s)$ versus log (UP) and selecting from these data, points which are dominated by strong-line absorptance. These points are then fitted to a surface obtained by plotting the log of the theoretical strong-line transmission function, τ_s, given by Eq. (11), versus the log of the quantity (CUP) versus the parameter n. The value of Log C may be obtained by taking the difference between Log (CUP) and Log (UP) from these two plots. The value of n may be obtained directly from the displacement along the n-axis. The correct values of n and C are obtained when the following expression is minimized:

$$\sum_{i=1}^{i=N} [\rho_i - f(n, D)]^2 \qquad (21)$$

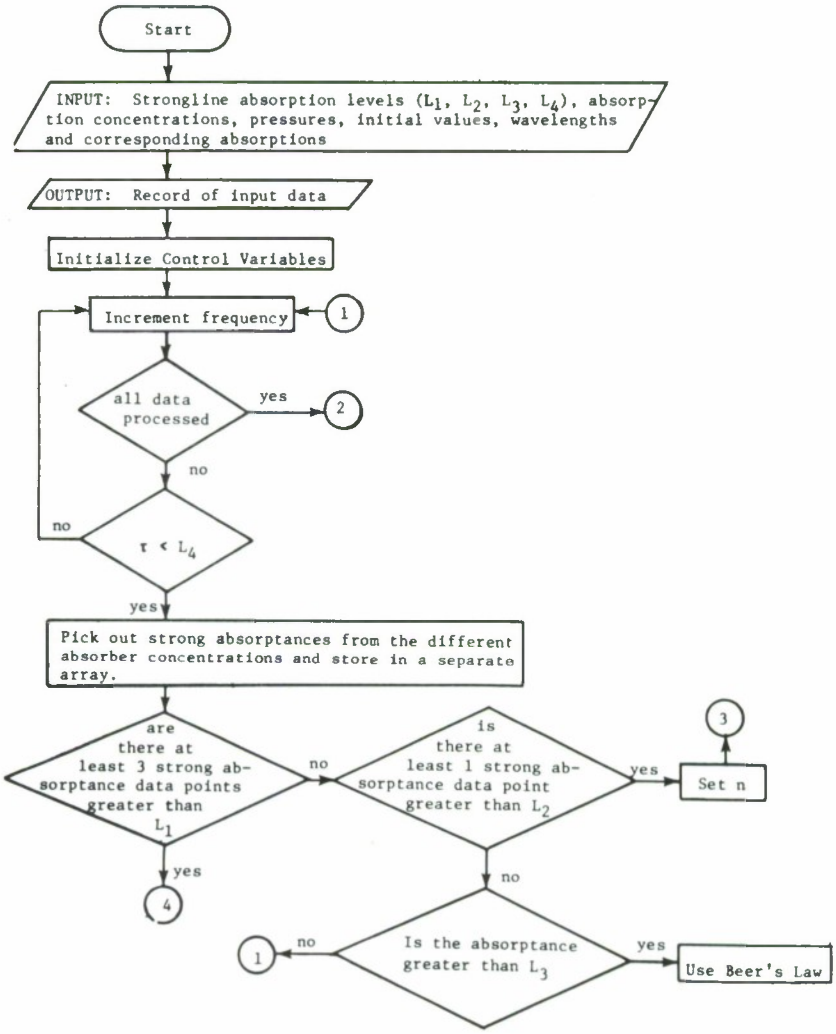

Figure 2. Flowchart of the five-parameter model.

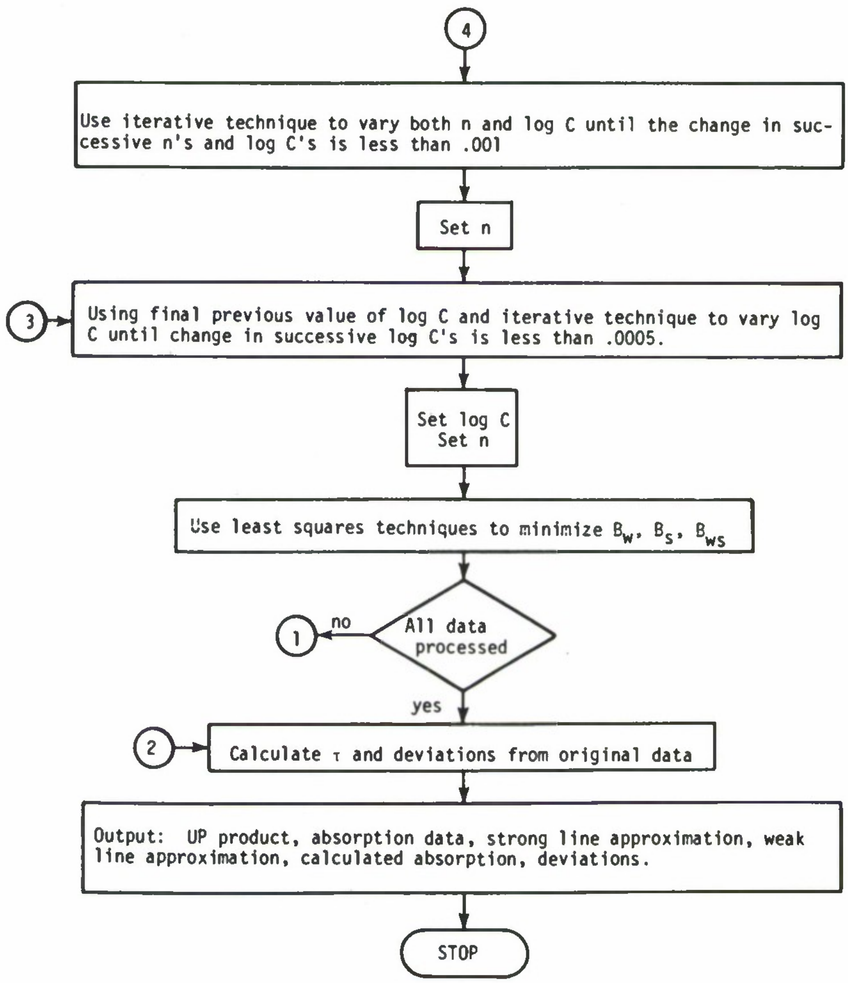
4
Use iterative technique to vary both n and log C until the change in successive n's and log C's is less than .001
Set n
3
Using final previous value of log C and iterative technique to vary log C until change in successive log C's is less than .0005.
Set log C
Set n
Use least squares techniques to minimize B_w, B_s, B_{ws}
no
1
All data processed
yes
2
Calculate τ and deviations from original data
Output: UP product, absorption data, strong line approximation, weak line approximation, calculated absorption, deviations.
STOP

Figure 2 (con.)

where D=Log C, $\rho_i = \log(1-\tau_i)$, $f(n, D) = \log(P\{n, [n\Gamma(n)(2CUP/\pi)^{\frac{1}{2}}]^{1/n}\})$, and N = the number of data points.

The data used in the calculation of the strong-line parameters were computer-selected by setting four levels of absorptance: L_1, L_2, L_3, and L_4. Levels L_1 and L_2 were used to determine which data would be used in the strong-line calculations (see Figure 2). Levels L_3 and L_4 were set to exclude values of absorptance near 0% and 100%, which in general are questionable. Small differences in these values may produce large errors in the parameters to be calculated. These levels were predetermined by trial and error, and it was found that the levels $L_1 = 0.5$, $L_2 = 0.2$, $L_3 = 0.005$, and $L_4 = 0.995$ produced the best parameters for water vapor.

First the data were checked against L_4; no values greater than L_4 were used. The data were next checked against L_1, and if there were at least three data points greater than L_1, then all of those points were used in the calculations. If there were not three points above L_1, then the data were checked with L_2. If there were three or more points above L_2, then those points were used; n was then set equal to a predetermined set value and Eq. (14) was minimized with respect to D only. This was necessary since minimization with respect to n and C was found to be difficult under these circumstances [13]. The selection of a value of n was made by a trial and error procedure, and a value of one was found to produce good parameters. If there were only one or two points above L_2, then the three highest absorptance values were used for the minimization with respect to D only. If there were no points above L_2, then the three highest absorptance values were used for the minimization with respect to D only. If there were no points above L_2, the absorption was assumed to be weak-line. The points between L_3 and L_2 were then selected and Beer's Law was used. B_s and B_{ws} were then set to zero and only B_w was calculated.

Since τ_s is nonlinear in n and D, the procedure used to minimize Eq. (14) was an iterative nonlinear technique. A modified Newton-Raphson method was used [14]; this expression was of the form

$$a_{k+1} = A_k + M_k^{-1} g(a_k) \tag{22}$$

where $g(a_k)$ is the set of equations obtained by taking the partial derivatives of Eq. (14) with respect to n and C, respectively, and setting them equal to zero, and M_k is the set of equations obtained by taking

$$\frac{\partial g(a_k)}{\partial n} \tag{23}$$

and

$$\frac{\partial g(a_k)}{\partial D} \tag{24}$$

The a_k's are

$$a_k = \begin{bmatrix} D_k \\ \vdots \\ \dot{n}_k \end{bmatrix} \qquad k = 0, 1, \ldots \tag{25}$$

The matrix obtained for $g(a_k)$ is

$$g(a_k) = \begin{bmatrix} \sum_{i=1}^{i=N} \dfrac{\overline{\partial f}^{\,i}}{\partial D} (\rho_i - \overset{i}{\bar{f}}) \\ \\ \sum_{i=1}^{i=N} \dfrac{\overline{\partial f}^{\,i}}{\partial n} (\rho_i - \overset{i}{\bar{f}}) \end{bmatrix} \qquad k = 0, 1, \ldots \tag{26}$$

The matrix M_k is obtained by expanding the function $f(n, D_i)$ in the Taylor series about the point (n, D_i), which makes f a minimum. The function can be closely approximated in the region of interest by considering only the linear terms in the Taylor series expansion of f. Using this simplifying approximation, we obtain

$$M_k = \begin{bmatrix} \sum_{i=1}^{i=N} \left(\overline{\frac{\partial f}{\partial D}}^{\,i}\right)^2 & \sum_{i=1}^{i=N} \left(\overline{\frac{\partial f}{\partial D}}^{\,i} \overline{\frac{\partial f}{\partial n}}^{\,i}\right) \\ \sum_{i=1}^{i=N} \left(\overline{\frac{\partial f}{\partial D}}^{\,i} \overline{\frac{\partial f}{\partial n}}^{\,i}\right) & \sum_{i=1}^{i=N} \left(\overline{\frac{\partial f}{\partial n}}^{\,i}\right)^2 \end{bmatrix} \qquad k = 0, 1, \ldots \tag{27}$$

where the symbol $\underline{i}$ indicates that the expression is evaluated at the point (n_j, D_j). The technique involved requires making an initial estimate of the values of n and D, then making successive guesses by incrementing n by no more than 0.1 and D by no more than 0.3 until successive a_k's are found such that their elements are less than 0.0005. When this difference is obtained, Eq. (14) is minimized with respect to n and D. In this procedure n is minimized first, and this value is used in minimizing D. In order for n and D to be minimized in this fashion, the initial estimates must be such that n and D can be determined within a limited number of iterations, which was arbitrarily chosen as 46 in the five-parameter computer program.

For the cases when n was set equal to 1.0 and Eq. (14) was minimized with respect to D only, Eqs. (26) and (27) became

$$g(a_k) = \left[\sum_{i=1}^{i=N} \frac{\partial f}{\partial D}^{i} (\rho_i - f) \right] \qquad k = 0, 1, \ldots \tag{28}$$

and

$$M_k = \left[\sum_{i=1}^{i=N} \left(\frac{\partial f}{\partial D}^{i} \right)^2 \right] \qquad k = 0, 1, \ldots \tag{29}$$

In order to determine the matrices for M_k and $g(a_k)$, the function f(n, D) and its partial derivatives with respect to n and D must be taken and evaluated. A series approximation method may be used to evaluate the incomplete gamma function; however, the function converges very slowly when it is close to the value 1. For this reason the (n, UP) plane was divided up into several areas of 50 points by 50 points. To approximate the log of the incomplete gamma function, a set of general third-order polynomials in n and log (CUP) was written in the form

$$\begin{aligned} f(n, x) = {} & A_1 x^3 + A_2 n x^2 + A_3 n^2 x + A_4 n^3 + A_5 x^2 \\ & + A_6 n x + A_7 n^2 + A_8 x + A_9 n + A_{10} \end{aligned} \tag{30}$$

where x = log (CUP). Tabulated values for the Incomplete gamma function were used [15], and Eq. (30) was fitted to those values by using least-squares techniques to determine the coefficients. These polynomials and their partials with respect to n and D were used in the calculation of $g(a_k)$ and M_k. A similar polynomial expression for the incomplete gamma function was also determined, since it must be evaluated in order to find values for τ_s. The functions were evaluated in the regions $0.5<n<3.0$ and $-4<\log(CUP)<4$. The polynomial approximations were within 0.001 of the actual values of the functions.

After the parameters n and C were determined, the quadratic parameters B_w, B_s, and B_{ws} were obtained by applying least-squares techniques to minimize the weighted difference between the theoretical Z_i^2 and the experimental Z_i^{*2}; i.e.,

$$\sum_{i=1}^{i=N} w(\tau_i^*)[B_w x_i^2 + B_s y_i^2 + B_{ws} x_i y_i - Z_i^{*2}]^2 \tag{31}$$

where $w(\tau_i^*) = \tau_i^{*2}(\ln\tau_i^*)^6$, and τ_i^* is the measured value of the transmission. This weighting function was postulated from the assumption that the transmittance is a random variable with a probability density

$$S = (\ln\tau)^{-2} \tag{32}$$

The variance of this density is proportional to $[\tau^{*2}(\ln\tau^*)^6]^{-1}$. In least-squares methods the weighting function is conventionally inversely proportional to the variance [16]. The expression for $w(\tau^*)$ is thus justified on this premise.

The procedure for minimizing Eq. (31) involves taking the partial derivatives with respect to B_w, B_s, and B_{ws} and setting them equal to zero. This yields three equations to be solved for these parameters:

$$\sum_{i=1}^{i=N} w(\tau_i^*)X_i^2(X_i^2 B_w + X_i Y_i B_{ws} + Y_i^2 B_s - Z_i^{*2}) = 0 \tag{33a}$$

$$\sum_{i=1}^{i=N} w(\tau_i^*)Y_i^2(X_i^2B_w + X_iY_iB_{ws} + Y_i^2B_s - Z_i^{*2}) = 0 \tag{33b}$$

$$\sum_{i=1}^{i=N} w(\tau_i^*)X_iY_i(X_i^2B_w + X_iY_iB_{ws} + Y_i^2B_s - Z_i^{*2}) = 0 \tag{33c}$$

The value of x_i is determined from I/U and the value of y_i is determined from the third-degree polynomial approximation for the incomplete gamma function. The above set of equations is easily solved at each frequency for the three quadratic parameters.

APPLICATION TO WATER VAPOR DATA AND COMPARISON TO AFCRL MODEL

The FP model was applied to the water vapor absorption data of Wyatt, Stull, and Plass [3] over absorption bands of 1200 to 2200 cm^{-1} and 4900 to 5800 cm^{-1} with a resolution of 50 cm^{-1}. The transmittances for the 1-km horizontal atmospheric path were calculated. The selection of this path resulted in an equivalent water vapor concentration of 2 pr-cm. The results of this application are represented by the solid lines in Figures 3 and 4.

The AFCRL model, described by McClatchey et al. [4], employs a modified King's function (MKF) as its molecular absorption model. It is an empirical model specifically tailored to fit a specific set of data for water vapor, carbon dioxide, ozone, and a combination of uniformly mixed gases (oxygen, methane, carbon monoxide, and nitrogenoxide). Since the AFCRL model has found use in GTS applications, a comparison between it and the FP model was made.

King [11] attempted to write a general expression for atmospheric transmittance (τ) which, under certain conditions, would approach either the strong-line or the weak-line approximation of either the Elsasser model or the Mayer-Goody model. He proposed that τ take the general functional form

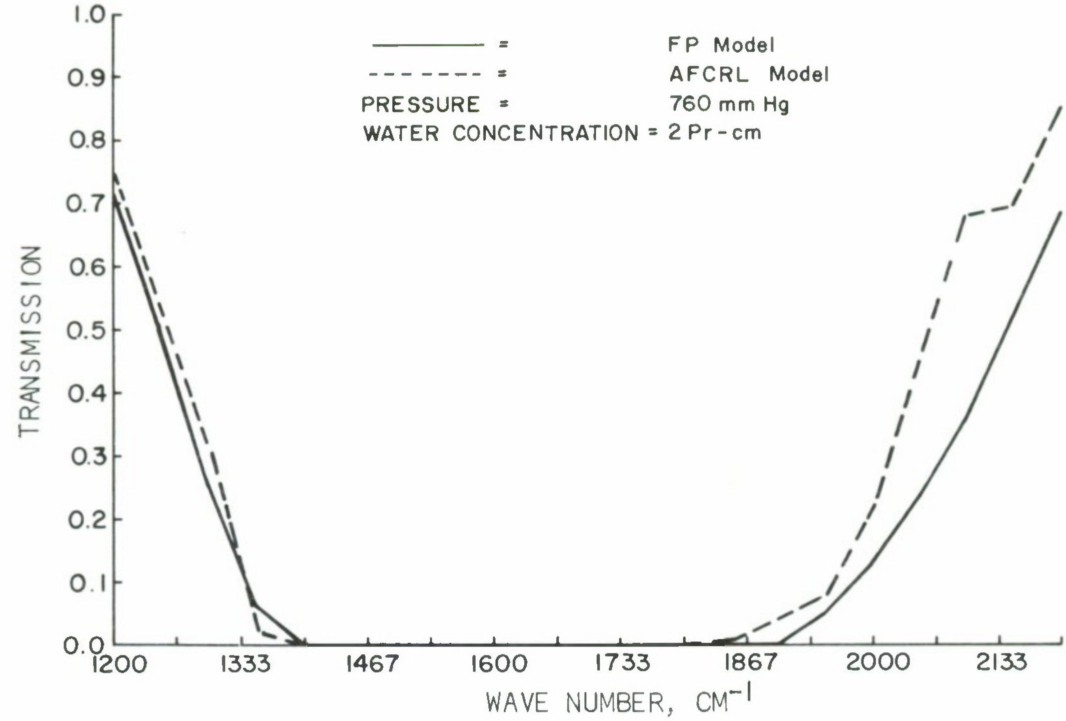

Figure 3. Comparison of the FP model with the AFCRL absorption model over the spectral interval 1200-2200 cm^{-1} with a resolution of 50 cm^{-1}.

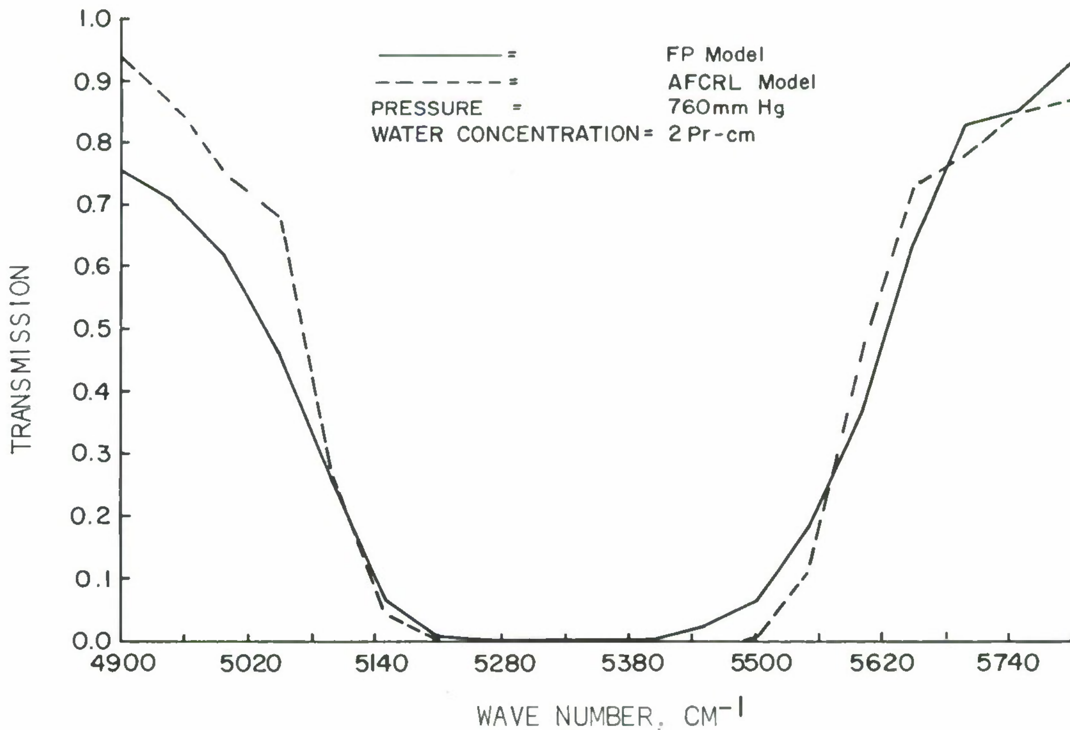

Figure 4. Comparison of the FP model with the AFCRL absorption model over the spectral interval 4900-5800 cm^{-1} with a resolution of 50 cm^{-1}.

$$\tau_{\Delta\nu}(\upsilon) = f[C(\upsilon)\ \Delta L P^n] \tag{34}$$

where

$\tau_{\Delta\nu}(\upsilon)$ = transmittance averaged over the spectral interval

$C(\upsilon)$ = frequency-dependent absorption coefficient

ΔL = optical path length

P = effective broadening pressure

n = frequency-dependent parameter

The King model is therefore a two-parameter model, with n and C as the frequency-dependent parameters. In the case of the MKF model, a mean value for n was determined graphically for a range of frequencies, thus reducing it to a one-parameter model [17].

In order to compare equivalent water concentrations for a 1-km horizontal path, the AFCRL tropical atmosphere model was chosen. The results are represented by the dashed lines in Figures 3 and 4.

In the 1200-2200 cm^{-1} band in Figure 3, we note that the two models predict generally similar though not identical results. In the region between 1850-2200 cm^{-1}, the two models differ significantly. In Figure 4 the two models differ in the region 4900-5100 cm^{-1}. In order to understand this difference, the input data must be examined.

Synthesized input data and experimentally measured data, both from Burch *et al.* [5], were used in the development of the MKF model. The data of Wyatt *et al.* [3] were obtained theoretically by calculating the absorptions due to spectral lines corresponding to transitions between various vibration-rotation energy levels. Discrepancies between experimental and theoretical data may be due to Wyatt's application of the equivalent symmetric rotor approximation to the highly asymmetric water molecule [4], since in the theoretical calculations it was necessary to assume that the water molecule was a symmetric rotator. Both sets of data are shown in Figures 5 and 6 (obtained from Wyatt *et al.*) for 1200-2200 cm^{-1} and 4900-5800 cm^{-1}, respectively.

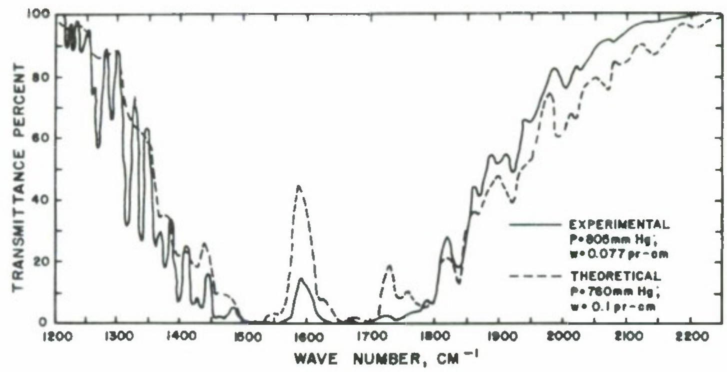

Figure 5. Comparison of the theoretical calculations of the transmittance of the 6.3 μ band with the experimental measurements of Burch et al. The theoretical values have been averaged over a 20 cm^{-1} interval.*

* Originally Figure 1 from [3].

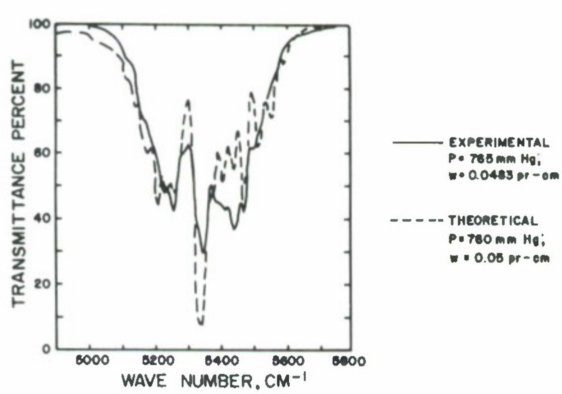

Figure 6. Comparison of the theoretical calculations of the transmittance of the 1.87 μ band with the experimental measurements of Burch et al. The theoretical values have been averaged over a 20 cm^{-1} interval.†

† Originally Figure 2 from [3].

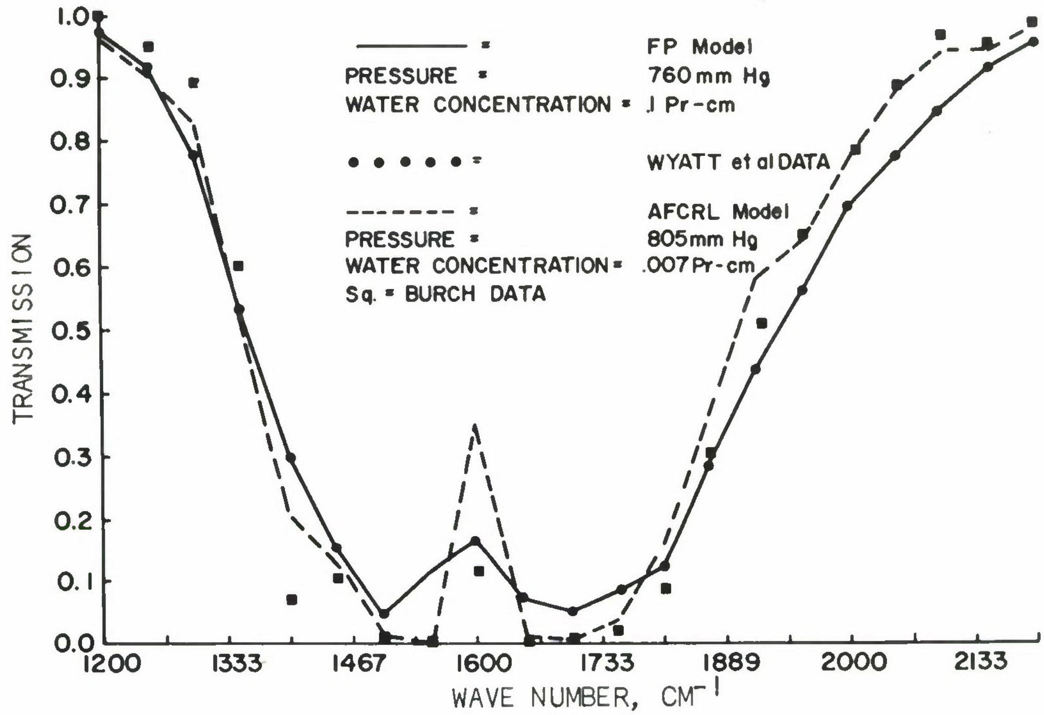

Figure 7. Comparison of the FP model to theoretical data of Wyatt et al., and comparison of the AFCRL model to empirical data of Burch over the spectral interval 1200-2200 cm^{-1} with a resolution of 50 cm^{-1}.

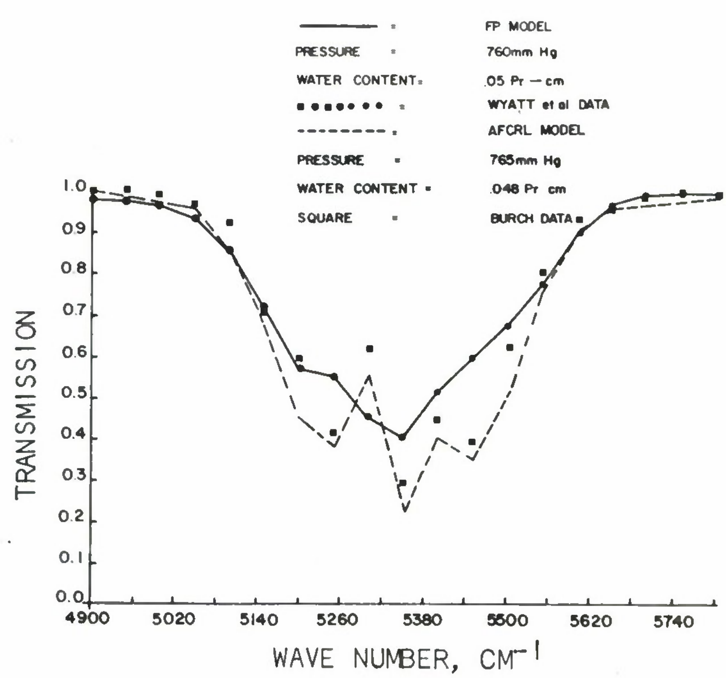

Figure 8. Comparison of the FP model to the theoretical data of Wyatt et al., and a comparison of the AFCRL model to the empirical data of Burch over the spectral interval 4900-5800 cm^{-1} with a resolution of 50 cm^{-1}.

A second comparison was then made between the results of the models and their respective data. The conditions for this comparison are as shown in Figures 5 and 6. The results are shown in Figures 7 and 8, where the solid line represents the results of the FP model and the dashed line that of the MKF model. The dots show the original Wyatt et al. data points, and the squares the published data of Burch et al. Tables 1 and 2 show the absolute deviation and give the RMS deviation of all points over each interval for both models. The RMS deviation for the 1200-2200 cm^{-1} band is 1.9×10^{-3} for the FP model and 71.3×10^{-3} for the MKF model; for the 4900-5800 cm^{-1} band, it is 1.7×10^{-3} for the five-parameter model and 48.2×10^{-3} for the MKF model. The FP model reproduced its data within 0.5% accuracy, while the MKF model, with the exception of three points, reproduced the published data of Burch et al. to within 10%.

CONCLUDING REMARKS

The addition of a fifth parameter to generalize the Zachor model, combined with the employment of high speed digital computers to accurately determine the parameters of the model by least-squares techniques and non-linear iteration methods, makes the five-parameter molecular absorption model a highly accurate and the most general analytical formula currently available. In contrast to empirical models, the five-parameter model also has the advantage of not being restricted to any particular set of data. Consequently, the five-parameter molecular absorption model is to be integrated into the Atmospheric Sciences Laboratory's (ASL) total atmospheric transmittance model.

In the 1200-2200 cm^{-1} band, the five-parameter model and the modified King's function model produce comparable though not identical results; in the 1850-2200 cm^{-1} region, they differ markedly. In the 4900-5800 cm^{-1} band they also predict similar results except in the 4900-5100 cm^{-1} region, where they again differ markedly. The results of the comparison between the five-parameter model and its input data and the modified King's function model and the published data of Burch et al. indicate that the former more accurately reproduces its data. To provide a more specific comparison, the two models need to be developed and applied to the same set of data over various atmospheric paths.

TABLE I

COMPARISON OF THE PREDICTIONS OF THE FIVE-PARAMETER ABSORPTION MODEL AND THE MODIFIED KING'S FUNCTION ABSORPTION MODEL WITH THEIR RESPECTIVE INPUT DATA OVER THE 1200-2200 cm^{-1} WATER VAPOR BAND

Wave Number	Wyatt et al. Data	FP Model	Absolute Deviation	Burch Data*	MKF Model*	Absolute Deviation*
1200	.972	.975	.003	.98	.96	.02
1250	.954	.955	.001	.94	.91	.03
1300	.781	.779	.002	.87	.83	.04
1350	.518	.521	.003	.60	.50	.10
1400	.299	.302	.003	.06	.20	.14
1450	.155	.155	.000	.10	.13	.03
1500	.047	.046	.001	.01	.01	.00
1550	.118	.114	.004	.00	.01	.01
1600	.165	.165	.000	.12	.36	.24
1650	.073	.070	.003	.00	.01	.01
1700	.052	.051	.001	.01	.01	.00
1750	.082	.083	.001	.02	.03	.01
1800	.123	.122	.001	.10	.16	.06
1850	.289	.290	.001	.30	.37	.07
1900	.435	.437	.002	.52	.58	.06
1950	.557	.559	.002	.65	.64	.01
2000	.691	.692	.001	.77	.77	.00
2050	.773	.773	.000	.89	.88	.01
2100	.850	.849	.001	.94	.94	.00
2150	.915	.914	.001	.96	.94	.02
2200	.957	.958	.001	.99	.98	.01

FP Model RMS Deviation = 1.9×10^{-3}

MKF Model RMS Deviation = 71.3×10^{-3}

*Only two significant figure accuracy was available for these data.

TABLE 2

COMPARISON OF THE PREDICTIONS OF THE FIVE-PARAMETER ABSORPTION MODEL AND THE MODIFIED KING'S FUNCTION ABSORPTION MODEL WITH THEIR RESPECTIVE INPUT DATA OVER THE 4900-5800 cm^{-1} WATER VAPOR BAND

Wave Number	Wyatt et al. Data	FP Model	Absolute Deviation	Burch Data*	MKF Model*	Absolute Deviation*
4900	.978	.979	.001	1.00	1.00	.00
4950	.976	.976	.000	1.00	.99	.01
5000	.965	.965	.000	.99	.97	.02
5050	.934	.935	.001	.97	.96	.01
5100	.858	.856	.001	.90	.85	.05
5150	.720	.717	.003	.71	.67	.04
5200	.571	.572	.001	.59	.45	.04
5250	.554	.556	.002	.42	.38	.04
5300	.411	.407	.004	.30	.22	.08
5400	.520	.521	.001	.44	.41	.03
5450	.599	.599	.000	.40	.35	.05
5500	.679	.680	.001	.63	.51	.14
5550	.770	.777	.002	.81	.76	.05
5600	.899	.899	.000	.94	.91	.03
5650	.970	.971	.001	.97	.97	.00
5700	.993	.994	.001	.99	.97	.02
5750	.995	.997	.002	1.00	.98	.02
5800	.998	.998	.000	1.00	.99	.01

FP Model RMS deviation = 1.7×10^{-3}

MKF Model RMS deviation = 48.2×10^{-3}

*Only two significant figure accuracy was available for these data.

Currently developmental work is being done for the ASL GTS modeling program (Contract Number DDAD07-73-C-0127) at the University of Texas at El Paso to extend the five-parameter model to real atmospheric conditions. This work consists of the application of inhomogeneous path techniques to the transmission calculations and the inclusion of transmission parameters for all important gaseous atmospheric constituents. The computer program efficiency will be maximized and the model will be applied to high resolution data.

Because of the large number of computations necessary to compute the five parameters, the model is best used over a limited spectral interval. However, if high accuracy is not required or if computer time and storage is limited, the completely developed program will have the capability of setting one or more of the parameters to a fixed value. This will result in reducing the five-parameter model to one of the nine models mentioned.

LITERATURE CITED

1. Gomez, R. B., and J. H. Pierluissi, "Atmospheric Effects for Ground Target Signature Modeling. III: Calculation Methods for Atmospheric Molecular Absorption," to be published as an ECOM report.

2. Zachor, A. S., 1968, "Equations for the Transmittance of the 2 CO_2 Bands," J. Quant. Spectrosc. Radiat. Transfer, 8, 1341-1349, Pergamon Press, 1518.

3. Wyatt, P. J., Robert Stull, and Gilbert N. Plass, 1964, "The Infrared Transmittance of Water Vapor," Applied Optics, 3, 229-241.

4. McClatchey, R. A., R. W. Fenn, J. E. A. Selby, F. E. Volz, and J. S. Garing, 1972, "Optical Properties of the Atmosphere," AFCRL-72-0497, Air Force Cambridge Research Laboratories, Air Force Systems Command, Bedford, Mass.

5. Burch, D. E., E. B. Singleton, W. L. France, and D. Williams, 1960, "Infrared Absorption by Carbon Dioxide, Water Vapor, and Minor Atmospheric Constituents," AF 19(604)-2633, Ohio State University.

6. Zachor, A. S., 1968, "A General Approximation for Gaseous Absorption," J. Quant. Spectrosc. Radiat. Transfer, 8, 771-781, Pergamon Press.

7. Gibson, G. A., and J. H. Pierluissi, 1971, "Accurate Formula for Gaseous Transmittance in the Infrared," Applied Optics, 10(7), 1509-1518.

8. Mayer, H., 1947, "Methods of Opacity Calculations," Los Alamos LA 647, Los Alamos, New Mexico.

9. Goody, R. N., 1952, "A Statistical Model for Water Vapor Absorption," Quart. J. Roy. Meteorol. Soc., 78, 165-169.

10. Pierluissi, J. H., 1973, "Polynomial Representation of Transmittance Models," Applied Optics, 12, 776-778.

11. King, J. I. F., 1964, "Band Absorption Model for Arbitrary Line Variance," J. Quant. Spectrosc. Radiat. Transfer, 4, 705-711, Pergamon Press.

12. Pierluissi, J. H., and R. B. Gomez, 1972, GTS Status Report.

13. Gibson, G. A., Private Communication, 5 April 1973.

14. Hildebrand, F. B., 1956, Chapters 7 and 10 of Introduction to Numerical Analysis, McGraw-Hill Book Co., Inc., New York.

15. Sims, R. J., 1970, "Strong-line Approximation for Gaseous Absorption," Electrical Engineering Report, University of Texas at El Paso, El Paso, Texas.

16. Deming, W. E., 1953, Chapters 4 and 8 of Statistical Adjustment of Data, Dover Press, New York.

17. Selby, J. E., Private Communication, 23 February 1973.

ATMOSPHERIC SCIENCES RESEARCH PAPERS

1. Dickson, David H., and James R. Oden, Fog Dissipation Techniques for Emergency Use, January 1972, ECOM-5420.
2. Pena, Ricardo, L. J. Rider, and Manuel Armendariz, Turbulence Characteristics at Heights of 1.5, 4.0, and 16.0 Meters at White Sands Missile Range, New Mexico, January 1972, ECOM-5421.
3. Miller, Walter B., On Calculation of Dynamic Error Parameters for the Rawinsonde and Related Systems, January 1972, ECOM-5422.
4. Richter, Thomas J., Rawin Radar Targets, February 1972, ECOM-5424.
5. Blanco, Abel J., and L. E. Traylor, Statistical Prediction of Impact Displacement due to the Wind Effect on an Unguided Artillery Rocket During Powered Flight, March 1972, ECOM-5427.
6. Williams, B. H., R. O. Olsen, and M. D. Kays, Stratospheric-Ionospheric Interaction During the Movement of a Planetary Wave in January 1967, March 1972, ECOM-5428.
7. Mason, J. B., and J. D. Lindberg, Laser Beam Behavior on a Long High Path, April 1972, ECOM-5430.
8. Dickson, D. H., Fogwash I An Experiment Using Helicopter Downwash, April 1972, ECOM-5431.
9. Schleusener, Stuart A., and Kenneth O. White, Applications of Dual Parameter Analyzers in Solid-State Laser Tests, April 1972, ECOM-5432.
10. Smith, Jack, Thomas H. Pries, Kenneth J. Skipka, and Marvin Hamiter, Optical Filter Function for a Folded Laser Path, April 1972, ECOM-5433.
11. Pries, Thomas H., Jack Smith, and Marvin Hamiter, Some Observations of Meteorological Effects on Optical Wave Propagation, April 1972, ECOM-5434.
12. Cantor, Israel, Survey of Studies of Atmospheric Transmission from a 4π Light Source to a 2π Receiver, April 1972, ECOM-5435.
13. Lowenthal, Marvin J., The Accuracy of Ballistic Density Departure Tables 1934-1972, April 1972, ECOM-5436.
14. Barr, William C., Accuracy Requirements for the Measurement of Meteorological Parameters Which Affect Artillery Fire, April 1972, ECOM-5437.
15. Duchon, C. E., F. V. Brock, M. Armendariz, and J. D. Horn, UVW Anemometer Dynamic Performance Study, May 1972, ECOM-5440.
16. Lee, Robert P., Artillery Sound Ranging Computer Simulations, May 1972, ECOM-5441.
17. Doswell, C. A., III, A Two-Dimensional Short-Range Fog Forecast Model, May 1972, ECOM-5443.
18. Doswell, C. A., III, An Iterative Method for Saturation Adjustment, June 1972, ECOM-5444.
19. Gomez, R. B., Atmospheric Effects for Ground Target Signature Modeling I. Atmospheric Transmission at 1.06 Micrometers, June 1972, ECOM-5445.
20. Bonner, R. S., A Technical Manual on the Characteristics and Operation of a Cloud Condensation Nuclei Collection/Detection/Recording Instrument, June 1972, ECOM-5447.
21. Waite, R. W., Reliability Test of Electronics Module of Meteorological Measuring Set AN/TMQ-22(XE-4), June 1972, ECOM-5448.
22. Horn, J. D., R. D. Reynolds, and T. H. Vonder Haar, Survey of Techniques Used in Display of Sequential Images Received from Geostationary Satellites, June 1972, ECOM-5450.
23. Collett, Edward, "Analysis of the Interaction of Partially Polarized Light with Dielectric Plates," ECOM-5451, July 1972 (AD 746 962).
24. Collett, Edward, "Mathematical Formulation of the Interference Laws of Freslen and Arago," ECOM-5452, July 1972 (AD 744 568).
25. Marchgraber, Reinhold M., "The Development of Standard Instruments for Radiation Measurements," ECOM-5453, July 1972 (AD 746 963).
26. Marchgraber, Reinhold M., "An Analogue Technique for the Improvement of the Frequency Response of a Thermal Radiometer," ECOM-5454, July 1972 (AD 747 049).

27. Bonner, R. S., and H. M. White, Microphysical Observations of Fog in Redwood Valley near Arcata-Eureka, California, July 1972, ECOM-5455.
28. Collett, E., and R. Alferness, "Depolarization of a Laser Beam in a Turbulent Medium," ECOM-5458, August 1972 (AD 747 886).
29. Cantor, Israel, and Michael Hudlow, Rainfall Effects on Satellite Communications in the K, X, and C Bands, July 1972, ECOM-5459.
30. Randhawa, J. S., Variations in Stratospheric Circulation and Ozone During Selected Periods, August 1972, ECOM-5460.
31. Seagraves, Mary Ann B., A General-Purpose Meteorological Rocket Data Reduction Program, August 1972, ECOM-5463.
32. Loveland, R. B., J. L. Johnson, and B. D. Hinds, Differential Magetic Measurements Near Cumulus Clouds, August 1972, ECOM-5463.
33. Nordquist, Walter S., Jr., and Dickson, David H., Helicopter Downwash Applied to Fog Clearing: A Status Summary, October 1972, ECOM-5465.
34. Rider, L. J., Armendariz, Manuel, Mean Horizontal Wind Speed and Direction Variability at Heights of 1.5 and 4.0 Meters Above Ground Level at WSMR, New Mexico, October 1972, ECOM-5466.
35. Engebos, Bernard F., Effects of Vertical Wind on Tactical Rockets and Artillery Shells, November 1972, ECOM-5467.
36. Armendariz, M., and James R. Scoggins, Characteristics of the Turbulent Diffusion Parameters as Related to Stability, November 1972, ECOM-5468.
37. White, Kenneth O., James B. Gillespie, Robert Armstrong, and Larry E. Traylor, State-of-the-Art Survey of Meteorological Instrumentation Required to Determine Atmospheric Effects on Airborne Laser Tests, November 1972, ECOM-5469.
38. Duncan, Louis D., and Barbara J. Richart, Mesoscale Variation of Spectral Radiance Near 15 Micrometers, December 1972, ECOM-5470.
39. Schleusener, Stuart A., and Kenneth O. White, Solid-State Laser Multiwavelength Identification and Display System, January 1973, ECOM-5473.
40. Nordquist, Walter S., Jr., Numerical Approximations of Selected Meteorological Parameters Related to Cloud Physics, March 1973, ECOM-5475.
41. Maynard, Harry, An Evaluation of Ten Fast Fourier Transform (FFT) Programs, March 1973, ECOM-5476.
42. Gerber, Hermann E., Freezing Water with Sized Agl Particles Part I: A Survey, March 1973, ECOM-5477.
43. Gerber, Hermann E., Freezing Water with Sized Agl Particles Part II: Theoretical Considerations, March 1973, ECOM-5478.
44. D'Arcy, Edward M., Accuracy Study of the T-9 Radar, March 1973, ECOM-5480.
45. Miller, Walter B., An Investigation of Errors Introduced into Meteorological Calculations Through Use of the Hypsometric Equation, April 1973, ECOM-5481.
46. Miller, Walter B., On Indirect Pressure Estimation from Measurements of Height and Temperature, April 1973, ECOM-5482.
47. Rinehart, G. S., and R. P. Lee, Apparent 7-Day Period in Visibility Data at White Sands Missile Range, New Mexico, April 1973, ECOM-5484.
48. Swingle, Donald M., and Raymond Bellucci, Improved Sound Ranging Location of Enemy Artillery, April 1973, ECOM-5486.
49. Lindberg, James D., and David G. Snyder, Determination of the Optical Absorption Coefficient of Powdered Materials Whose Particle Size Distribution and Refractive Indices Are Not Known, April 1973, ECOM-5487.
50. Rubio, Roberto, "Winter Anomalous Radio Wave Absorption Days at 32° N Latitude and Prevalent Solar Radiation," ECOM-5488, May 1973.
51. Nordquist, W. S., "Data from a Fog Dispersal Experiment Using Helicopter Downwash," ECOM-5456, May 1973.
52. Shinn, Joseph H., "Optimum Wind Soundings and Army Fallout Prediction Accuracies," ECOM-5489, May 1973.
53. Miller, Walter B., and Donald R. Veazey, "An Integrated Error Description of Active and Passive Balloon Tracking Systems," ECOM-5500, June 1973.
54. Doll, Barry, "The Potential Use of Polarized Reflected Light in the Remote Sensing of Soil Moisture," ECOM-5501, July 1973.

55. Duncan, Louis D., "A Geometric Investigation of the Effect of Viewing Angle on the Ground Resolution of Satellite-Borne Sensors," ECOM-5502, July 1973.

56. Miller, Walter B., and Donald R. Veazey, "Vertical Efficiency of Active and Passive Balloon Tracking Systems from a Standpoint of Integrated Error," ECOM-5503, August 1973.

57. Richter, Thomas J., "Design Considerations for the Calculator, Altitude ML-646(XE-1)/UM," ECOM-5504, August 1973.

58. Randhawa, J. S., "Measurement of Total Ozone at WSMR, NM," ECOM-5505, August 1973.

59. Mason, James B., "Lidar Measurement of Temperature: A New Approach," ECOM-5506, August 1973.

60. Randhawa, J. S., "An Investigation of Solar Eclipse Effect on the Subpolar Stratosphere," ECOM-5507, September 1973.

61. Wade, Gerald T., Teddy L. Barber, and Robert Armstrong, "A Proposed Versatile Photon Counter System for Laser Radar," ECOM-5508, September 1973.

62. Lentz, W. J., "A New Method of Computing Spherical Bessel Functions of Complex Argument with Tables," ECOM-5509, September 1973.

63. White, Kenneth O., Gerald T. Wade, and Stuart A. Schleusener, "The Application of Minicomputers in Laser Atmospheric Experiments," ECOM-5510, September 1973.

64. Collett, E., R. Alferness, and T. Forbes, "Log-Intensity Correlations of a Laser Beam in a Turbulent Medium," ECOM-5511, September 1973.

65. Robbiani, Raymond L., "Design Concept of a Forward Area Rawinsonde set (FARS)," ECOM-5512, October 1973.

66. Stone, William J., "The Hydrometeorologic Ground Truth Facility at White Sands Missile Range, New Mexico," ECOM-5513, October 1973.

67. Lacy, Claud H., "Objective Analysis Using Modeled Space-Time Covariances: An Evaluation," ECOM-5514, October 1973.

68. Stipanuk, G. S., "Algorithms for Generating a SKEW-T, log p DIAGRAM and Computing Selected Meteorological Quantities," ECOM-5515, October 1973.

69. Sharenow, Moses, "Test and Evaluation of Natural Rubber Spherical Balloons," ECOM-5516, October 1973.

70. White, Kenneth O., and Gerald T. Wade, "Remote Sensing of Atmospheric Methane Using an Erbium/YAG Laser: A Feasibility Study," ECOM-5517, November 1973.

71. Tchen, Chan Mou, and Edward Collett, "The Spectrum of Laser-Induced Turbulence," ECOM-5518, November 1973.

72. Collett, Edward, and Chan Mou Tchen, "Turbulent Heating of an Atmosphere by a Laser Beam," ECOM-5519, November 1973.

73. Gerber, Hermann E., "Freezing Water with Sized AgI Particles. Part III: Experimental Procedure, Results, and Conclusions," ECOM-5520, November 1973.

74. Lindberg, James D., "A Simple Method for Measuring Absolute Diffuse Reflectance with a Laboratory Spectrophotometer," ECOM-5521, November 1973.

75. Lindberg, James D., and Michael S. Smith, "Visible and Near Infrared Absorption Coefficients of Kaolinite and Related Clays," ECOM-5522, November 1973.

76. Weathers, L. R., and R. B. Loveland, "Magnetic Field Survey at White Sands Missile Range, New Mexico," ECOM-5523, November 1973.

77. Matonis, Casimir J., "The Potential Use of Tactical Microwave Radio (TMR) for Transmission of Weather Radar Data," ECOM-5524, December 1973.

78. Lindberg, James D., and Laude, Larry S., "A Measurement of the Absorption Coefficient of Atmospheric Dust," ECOM-5525, December 1973.

79. Low, Richard D. H., "Microphysical and Meteorological Measurements of Fog Supersaturation," ECOM-5526, December 1973.

80. Nordquist, Walter S., "Fog Clearing Using Helicopter Downdrafts: A Numerical Model," ECOM-5527, December 1973.

81. Lentz, W. J., and G. B. Hoidale, "Estimates of the Extinction of Electromagnetic Energy in the 8 to 12 μm Range by Natural Atmospheric Particulate Matter," ECOM-5528, January 1974.

82. Duncan, Louis D., and Marvin Kays, "Determining Nuclear Fallout Winds from Satellite-Observed Spectral Radiances," ECOM-5529, January 1974.
83. Henley, David C., "An Analysis of Random Fluctuations of Atmospheric Dust Concentrations," ECOM-5530, January 1974.
84. Gillespie, James B., and Carmine Petracca, "Atmospheric Effects for Ground Target Signature Modeling. II. Discussion and Application of a Generalized Molecular Absorption Model," ECOM-5531, January 1974.

DISTRIBUTION LIST

Commanding Officer
Picatinny Arsenal
ATTN: SMUPA-VA6, Bldg 59
Dover, NJ 07801
2

Chief, Analytical Sci Off
Biological Def Rsch Lab
ATTN: AMXBL-AS
Dugway, Utah 84022

Commanding Officer
Fort Detrick
ATTN. Tech Library
SMUFD-AE-T
Frederick, MD 21701

Commanding Officer
Edgewood Arsenal
ATTN: SMUEA-TSTI-TL
Edgewood Arsenal, MD 21010

Commanding Officer
US Army Nuclear Def Lab
ATTN: Library
Edgewood Arsenal, MD 21010
2

Commanding Officer
Aberdeen Proving Ground
ATTN: Tech Lib, Bldg 313
Aberdeen Proving Ground, MD 21005
2

Commanding Officer
US Army Ballistics Rsch Lab
ATTN: Tech Info Div
Aberdeen Proving Ground, MD 21005

Dir of Meteorological Sys
Office of Applications (FM)
Natl Aero & Space Admin
Washington, D. C. 20546

Director
US Weather Bureau
ATTN: Librarian
Washington, D. C. 20235

Dr. A. D. Belmont
Research Div
Control Data Corp
Minneapolis, Minn 55440

Chief, Aerospace Environ Div
CODE S&E-AERO-Y
NASA
Marshall Space Flight Center, Alabama 35802

Commandant
US Army Field Artillery School
ATTN: ATSFA-G-RA-RK
Ft. Sill, OK 73503

Technical Library
WSMR, New Mexico 88002
3

Natl Aeronautics & Space Admin
George C Marshall Space Flight Center
Aero-Astrodynamics Laboratory
ATTN: S&E-AERO-YS/Mr. D. Camp
Marshall Space Flight Center, Alabama 35812

Dr. F. de Percin
Chief, Atmospheric Sci Branch
Environmental Sciences Division
US Army Research Office
3045 Columbia Pike
Arlington, VA 22204

Geophysics Officer
Code 3250
Pacific Missile Range
Point Mugu, CA 93042

US Army Liaison Office
MIT, Bldg 26, Rm 131
77 Massachusetts Avenue
Cambridge, Mass 02139

The Library of Congress
ATTN: Exchange & Gift Div
Washington, D. C. 20540
2

Head, Atmospheric Sci Section
National Science Foundation
1800 G Street, N.W.
Washington, D. C. 20550

Director, Systems R&D Service
Federal Aviation Admin
800 Independence Avenue S.W.
Washington, D. C. 20590

Technical Processes Br - D823
Room 806, Libraries Div - NOAA
8060 13th Street
Silver Spring, MD 20910

William A. Main
USDA Forest Service
215 Natural Resources Building
Michigan State University
East Lansing, Mich 48823

NASA Headquarters
Meteorology & Sounding Branch
(CODE SAM)
Space Applications Programs
Washington, D. C. 20546

Chief, Fallout Studies Branch
Division of Biology & Medicine
Atomic Energy Commission
Washington, D. C. 20545

Director
Atmospheric Physics & Chem Lab
Room 31
NOAA Dept of Commerce
Boulder, Colorado 80302

Natl Center for Atmos Research
NCAR Library, Acquisitions-Rept
Boulder, Colorado 80302

E&R Center, Bureau of Reclamation
ATTN: D-751, Bldg 67
Denver, Colorado 80225

Natl Oceanographic Data Center - D722
Natl Oceanic & Atmos Admin
US Dept of Commerce
Rockville, MD 20852

Institute of Sci & Technology
The University of Michigan
Box 618, (IRIA Library)
Ann Arbor, Mich 48107

NASA Scientific & Tech Info Fac
ATTN: Acquisitions Br (S-AK/DL)
P. O. Box 33
College Park, MD 20740
2

Battelle Memorial Institute
Strategic Technology Office
Information Analysis Center
505 King Avenue
Columbus, Ohio 43201

Infrared Info & Analysis Center
University of Michigan
Institute of Science & Technology
Box 618
Ann Arbor, Mich 48107

VELA Seismic Info Center
University of Michigan
Box 618
Ann Arbor, Mich 48107

Commanding General
US Army Elect Command
ATTN: AMSEL-RD-LNF
Ft Monmouth, NJ 07703

Commanding Officer
US Army Engineer Topographic Labs
Ft Belvoir, VA 22060

CO, USA Foreign Sci & Tech Center
ATTN: AMXST-ISI
220 7th Street, NE
Charlottesville, VA 22901

Commanding General
US Army Elect Command
ATTN: AMSEL-BL
Ft Monmouth, NJ 07703
3

Commanding General
US Army Elect Command
ATTN: AMSEL-BL-AP
Ft Monmouth, NJ 07703

Commanding General
US Army Elect Command
ATTN: AMSEL-BL-TE
Ft Monmouth, NJ 07703

Commanding General
US Army Elect Command
ATTN: AMSEL-BL-FM-A
Ft Monmouth, NJ 07703

Environmental Protection Agency
Division of Meteorology
Research Triangle Park, North Carolina 27711

Commandant
US Army Field Artillery School
ATTN: Dept of Target Acquisition
Ft Sill, OK 73503

Commandant
US Army Field Artillery School
ATTN: Met. Division
Ft Sill, OK 73503

Armament Dev & Test Center
ADTC(DLOSL)
Eglin AFB, FL 32542

Gary D. Atkinson, LtC USAF
Chief, Technical Services Div
DCS/Aerospace Sciences
ATTN: AWS/DNTI
Scott AFB, IL 62225

Director
National Security Agcy
ATTN: TDL
Ft George G Meade, MD 20755

Commander, Naval Ship Sys Command
Tech Library, RM 3 S-08
Washington, D. C. 20360

Commander
Naval Weather Ser Command
Washington Navy Yard (Bldg 200)
Washington, D. C. 20390

Commanding Officer
Harry Diamond Laboratory
ATTN: Library
Washington, D. C. 20438

Rome Air Devel Center
ATTN: Documents Library (TDLD)
Griffiss AFB, NY 13440

Air Force Cambridge Rsch Labs
ATTN: LC(1124)
L. G. Hanscom Field
Bedford, Massachusetts 01730

Air Force Avionics Laboratory
ATTN: AFAL/DOT, STINFO
Wright-Patterson AFB, Ohio 45433
2

HQ, AFCS(EICRW)
Richards-Gebaur AFB, MO 64030

Ofc of Asst Ch of Staff for Intelligence
Dept of the Army
ATTN: ACSI-DD
Washington, D. C. 20310
2

Commanding General
US Army Materiel Command
ATTN: AMCRD-H
Washington, D. C. 20315

Commanding General
US Army Missile Command
ATTN: AMSMI-RR, Dr. J. P. Hallowes
Redstone Arsenal, Alabama 35809

CG, US Army Missile Cmd
Redstone Scientific Info Center
ATTN: Chief, Document Section
Redstone Arsenal, Alabama 35809
2

Commanding General
US Army Test & Eval Cmd
ATTN: NBC Directorate
Aberdeen Proving Ground, MD 21005

Commanding Officer
USACDC FAA
Ft Sill, OK 73503

Commanding Officer
Frankford Arsenal
ATTN: Library, H1300, Bl. 51-2
Philadelphia, PA 19137

Commanding Officer
Frankford Arsenal
ATTN: W1000-65-1 (Mr. Helfrich)
Philadelphia, PA 19137

Commanding Officer
USASA Test & Eval Cen
Ft Huachuca, Arizona 85613

Commanding Officer & Dir
US Navy Ele Lab
ATTN: Library
San Diego, CA 92152

Commander
US Naval Ordnance Lab
ATTN: Tech Library
White Oak, Silver Spring, MD 20910

Commander
Naval Elect Sys Cmd HQ
ATTN: CODE 05611
Washington, D. C. 20360

Commandant, Marine Corps
HQ, US Marine Corps
ATTN: CODE A04C
Washington, D. C. 20380

Marine Corps Dev & Educ Cmd
Development Center
ATTN: C-E Div
Quantico, VA 22134

Commander
US Naval Weapons Lab
ATTN: KEB-2F(FENN)
Dahlgren, VA 22448

Commander, Naval Air Sys Command
Meteorological Div (AIR-540)
Washington, D. C. 20360

Air Force Cambridge Rsch Labs
ATTN: LKI
L. G. Hanscom Field
Bedford, Mass. 01730
2

AFCRL (LYV)
L. G. Hanscom Field
Bedford, Mass. 01730

HQ, Elect Sys Div (TRI)
L. G. Hanscom Field
Bedford, Mass. 01730

Recon Central/RSA
AF Avionics Lab
Wright-Patterson AFB, Ohio 45433

HQ, Air Weather Service
ATTN: AWVAS/TF (R. G. Stone)
Scott AFB, IL 62225

US Air Force Security Ser
ATTN: TSG
San Antonio, TX 78241

HQ, Air Force Sys Command
ATTN: DLTE
Andrews AFB, MD 20331

Air Force Weapons Lab
ATTN: WLIL
Kirtland AFB, NM 87117

Ofc of Asst Ch of Staff for DS-SSS
Dept of the Army
Rm 3C466, The Pentagon
Washington, D. C. 20315

Ofc Asst Sec of the Army (R&D)
ATTN: Asst for Research
Rm 3-E-379, The Pentagon
Washington, D. C. 20310

Chief of Rsch & Development
ATTN: CRDES
Washington, D. C. 20315
2

Commanding General
US Army Materiel Command
ATTN: AMCMA-EE
Washington, D. C. 20315

Commanding General
US Army Materiel Command
ATTN: AMCRD-TV
Washington, D. C. 20315
2

Commanding General
US Army Missile Command
ATTN: AMSMI-RRA, Bldg 7770
Redstone Arsenal, AL 35809

CG, US Army Missile Command
Redstone Scientific Info Cen
ATTN: Chief, Document Section
Redstone Arsenal, AL 35809
3

Commanding General
US Army Combat Devel Command
Intelligence & Control Sys Gr.
ATTN: INCSCSD-C
Ft Belvoir, VA 22060
2

Commanding Officer
US Army Limited War. Lab
ATTN: CRDLWL-7C
Aberdeen Proving Ground, MD 21005

Director
US Army Ballistic Lab
ATTN: AMXRD-BSP (Dr. Reuyl)
Aberdeen Proving Ground, MD 21005

Commanding General
US Army Test & Eval Command
ATTN: AMSTE-EL
Aberdeen Proving Ground, MD 21005

Commanding General
US Army Test & Eval Command
ATTN: AMSTE-FA
Aberdeen Proving Ground, MD 21005

Commanding General
US Army Test & Eval Command
ATTN: AMSTE-NBC
Aberdeen Proving Ground, MD 21005

Commanding General
US Army Munitions Cmd
ATTN: AMSMU-RE-R
Dover, NJ 07801

Director
US Army Munitions Command
Operations Research Group
Aberdeen Proving Ground, MD 21010

Commanding General
US Army Munitions Command
ATTN: AMSMU-RE-P
Dover, NJ 07801

Commanding Officer
Picatinny Arsenal
ATTN: SMUPA-TVI
Dover, NJ 07801

Commanding Officer
USA Garrison
ATTN: Tech Ref. Div.
Fort Huachuca, Arizona 85613

Chief, A.M. & EW Division
ATTN: USAEPG-STEEP-TD
Fort Huachuca, Arizona 85613

US Army Rsch. Off. - Durham
Box CM, DUKE Station
ATTN: CRDARD-IP
Durham, N. Carolina 27706

USA Security Agcy Combat Dev Actv
ATTN: IACDA-P(T) & IACDA-P(L)
Arlington Hall Station, Bldg 420
Arlington, Virginia 22212
2

Technical Support Directorate
ATTN: Technical Library
Bldg 3330
Edgewood Arsenal, MD 26010

Commandant
US Army Chemical Cen & School
Micromet. Section (Chem. Br.)
Ft McClellan, Ala 36201

Director
USA Engr Waterways Exper Sta
ATTN: Rsch Center Library
Vicksburg, Mississippi 39180
2

CG, Deseret Test Center
ATTN: STEPD-TT-ME(S) MET DIV
Bldg 103, Soldiers Circle
Fort Douglas, Utah 84113

Commanding General
USA CDC Combat Arms Group
Ft. Leavenworth, Kansas 66027

Commanding Officer
Eustis Directorate
US Army Air Mobility R&D Lab
ATTN: Technical Library
Fort Eustis, VA 23604

Director, US Army Advanced Matl Concepts Agcy
ATTN: AMXAM
Washington, D. C. 20315

Commanding Officer
USACDC CBR Agcy
Ft. McClellan, Ala 36201

Commanding General
US Army Materiel Command
ATTN: AMCRD R (H. Cohen)
Washington, D. C. 20315

Commanding Officer
US Army Combat Dev Cmd
Communications-Elect Agcy
Ft Monmouth, NJ 07703

US Army Liaison Office
MIT-Lincoln Lab, Rm A-210
P. O. Box 73
Lexington, Mass. 02173

HQ, US Army Combat Dev Cmd
ATTN: CDCLN-EL
Ft Belvoir, VA 22060

Commanding General
US Army Tank-Automotive Cmd
ATTN: AMSTA-Z, Mr. R. McGregor
Warren, Michigan 48090

Commanding General
US Army Elect Command
ATTN: AMSEL-GG-TD
Ft Monmouth, NJ 07703
2

Commanding General
US Army Elect Command
ATTN: AMSEL-EW
Ft Monmouth, NJ 07703

Commanding General
US Army Elect Command
ATTN: AMSEL-ME-NMP-PS
Ft Monmouth, NJ 07703

Commanding General
US Army Elect Command
ATTN: AMSEL-MS-TI
Ft Monmouth, NJ 07703

Commanding General
US Army Elect Command
ATTN: AMSEL-XL-D
Ft Monmouth, NJ 07703

Commanding General
US Army Elect Command
ATTN: AMSEL-WL-D
Ft Monmouth, NJ 07703

Commanding General
US Army Elect Command
ATTN: AMSEL-NL-D
Ft Monmouth, NJ 07703

Commanding General
US Army Elect Command
ATTN: AMSEL-KL-D
Ft Monmouth, NJ 07703

Commanding General
US Army Elect Command
ATTN: AMSEL-VL-D
Ft Monmouth, NJ 07703

Commanding General
US Army Elect Command
ATTN: AMSEL-CT-D
Ft Monmouth, NJ 07703
3

Commanding General
US Army Elect Command
ATTN: AMSEL-SC
Ft Monmouth, NJ 07703

Commanding General
US Army Elect Command
ATTN: AMSEL-RD-D
Ft Monmouth, NJ 07703

Commanding General
US Army Combat Dev Cmd
ATTN: CDCMR-E
Ft Belvoir, VA 22060

President
US Army Artillery Board
Ft Sill, OK 73503

Dir of Defense Rsch & Engin
ATTN: Tech Library
RM 3E-1039, The Pentagon
Washington, D. C. 20301

Defense Intelligence Agcy
ATTN: DIAAP-10A2
Washington, D. C. 20301

Director, Defense Nuclear Agency
ATTN: Tech Library
Washington, D. C. 20305

Naval Ships Systems Command
ATTN: CODE 20526 (Tech Lib)
Main Navy Bldg, Rm 1528
Washington, D. C. 20325

Director
US Naval Rsch Laboratory
ATTN: CODE 2627
Washington, D. C. 20390
2

CO, Edgewood Arsenal
Defense Devel & Engineering Lab
ATTN: SMUEA-DDW-2, Mr. H. Tannenbaum
Edgewood Arsenal, MD 21010

Commanding Officer
Aberdeen Proving Ground
ATTN: STEAP-TL
Aberdeen Proving Ground, MD 21002

Director, Ballistic Rsch Labs
US Army Aberdeen Rsch & Dev Cen
ATTN: AMXRD-BTL, Mr. F. J. Allen
Aberdeen Proving Ground, MD 21005

Commanding Officer
US Army Ballistic Rsch Labs
ATTN: AMXBR-B & AMXBR-1A
Aberdeen Proving Ground, MD 21005
2

Commanding Officer
US Army Land Warfare Lab
ATTN: CRDLWL-4A
Aberdeen Proving Ground, MD 21005

Commanding Officer
US Army Elect Proving Ground
ATTN: STEEP-MT-EA
Ft Huachuca, Arizona 85613

Commanding Officer
US Army Dugway Proving Ground Library
ATTN: STEDP-TL, Tech Library
Dugway, Utah 84022

Commanding Officer
US Army Cold Regions R&E Lab
ATTN: CRREL-RP (Dr. Yin Chao Yen)
Hanover, New Hampshire 03755

Commanding Officer
Yuma Proving Ground
ATTN: STEYP-AD(TECH LIBRARY)
Yuma, Arizona 85364

Commanding Officer
US Army Arctic Test Center
APO Seattle 98733
2

CO, US Army Tropic Test Center
ATTN: STETC-AD-TL
APO New York 09827
2

Commanding Officer
USACDC Inst of Nuclear Studies
Ft Bliss, TX 79916

Commanding Officer
USADDC Inst of Systems Analysis
ATTN: CDISA-SSCI & CDISA-STANO
Ft Belvoir, VA 22060

Commanding General
US Army Missile Command
ATTN: AMSMI-RFG, Mr. N. Bell
Redstone Arsenal, AL 35809

Commanding Officer
Frankford Arsenal
ATTN: SMUFA-N-5300, Mr. M. Schoenfield
Bldg 201
Philadelphia, PA 19137

Commanding Officer
US Army Satellite Comm Agcy
ATTN: AMCPM-SC-3
Ft Monmouth, NJ 07703

Director
Night Vision Lab (USAECOM)
ATTN: ASMEL-NV-OR, Mr. S. Segal
Ft Belvoir, VA 22060

Sylvania Elect Sys-Western Div
ATTN: Technical Reports Lib
P. O. Box 205
Mountain View, CA 94040

NASA HEADQUARTERS
Prg. Ch, MET & Soundings (SRM)
Earth Observations Programs
Washington, D. C. 20546

Library-R51-Tech Reports
Environmental Research Labs
NOAA
Boulder, Colorado, 80302

Commandant
US Army Air Defense School
ATTN: C&S Dept, MSL SCI DIV
Ft Bliss, TX 79916

Defense Documentation Center
ATTN: DDC-TCA
Cameron Station (Bldg 5)
Alexandria, VA 22314
12

Director, USN Research Lab.
ATTN: Code 6530, H. Shenker
Washington, D. C. 20390

Mr. E. F. Corwin
Head, Met Research Branch
Meteorological Division
Naval Air Sys Cmd (AIR-5401)
Washington, D. C. 20360

Commanding Officer
US Army Combat Dev Cmd
Intelligency Agency
ATTN: CDCINT-P, Cpt Thoresen
Ft. Huachuca, Arizona

Director
US Army Advanced Materiel Concepts Agency
2461 Eisenhower Avenue
Alexandria, VA 22314

University of Oklahoma
Research Institute
Field Artillery Research Off
P. O. Box 3124
Ft. Sill, OK 73503

Dir US Naval Research Lab
ATTN: CODE 6530, H. Shenker
Washington, D. C. 20390

DEPARTMENT OF THE ARMY
ATMOSPHERIC SCIENCES LABORATORY
US ARMY ELECTRONICS COMMAND
AMSEL-BL-DP-P
WHITE SANDS MISSILE RANGE
NEW MEXICO 88002

OFFICIAL BUSINESS
Penalty For Private Use, $300

POSTAGE AND FEES PAID
DEPARTMENT OF THE ARMY
DoD 314

U.S. MAIL

Air Force Weapons Lab
ATTN: WLIL
Kirtland AFB, NM 87117